Available online at www.sciencedirect.com
ScienceDirect
Polymer 48 (2007) 2046–2055
polymer
www.elsevier.com/locate/polymer

Thermally stable NLO poly(amide–imide)s via sequential self-repetitive reaction

Huey-Ling Chang [a,*], Hsun-Lien Lin [b], Yi-Chia Wang [b], Shenghong A. Dai [b], Wen-Chiung Su [c], Ru-Jong Jeng [b,**]

[a] *Department of Chemical and Materials Engineering, National Chinyi University of Technology, Taichung 411, Taiwan*
[b] *Department of Chemical Engineering, National Chung Hsing University, 250 Kuo-Kuang Road, Taichung 402, Taiwan*
[c] *Chung-Shan Institute of Science and Technology, Lungtan, Tauyuan 325, Taiwan*

Received 29 July 2006; received in revised form 6 February 2007; accepted 8 February 2007
Available online 12 February 2007

Abstract

A series of thermally stable side-chain second-order nonlinear optical (NLO) poly(amide–imide)s via sequential self-repetitive reaction (SSRR) have been developed. This SSRR is based on carbodiimide (CDI) chemistry. Three difunctional azo chromophores (DR19, NDPD and DNDA) were, respectively, reacted with excessive amount of 4,4′-methylene-diphenylisocyanate (MDI) to form poly-CDI, and subsequently trimellitic anhydride (TMA) was added to obtain an intermediate, poly(*N*-acylurea). Poly(*N*-acylurea) exhibits excellent organosolubility, which enables the fabrication of high quality optical thin films. Moreover, its moderate glass transition temperature (T_g) characteristic allows the NLO-active polymer to exhibit high poling efficiency. After in situ poling and curing process, *N*-acylurea moieties were converted to amide–imide structures via SSRR, and the T_gs of the polymers were elevated significantly up to 70 °C higher than that of the poly-CDI sample. Electro-optical coefficients, r_{33} of about 5.2–25.2 pm/V at 830 nm were obtained. Good temporal stability (80 °C) and waveguide optical losses (3.8–6.6 dB/cm at 830 nm) were also obtained for these polymers.

Keywords: Poly(amide–imide); Sequential self-repetitive reaction; NLO

1. Introduction

Organic polymeric second-order nonlinear optical (NLO) materials have been of great interest for many years due to their potential applications in photonic devices [1–5]. These materials exhibit large susceptibilities and fast response times, and are agreeable to molecular modification [6]. The key requirements imposed on the NLO polymers include large optical nonlinearities and temporal stability at 80–125 °C. For NLO polymers utilizing an electric field to achieve the orientation of chromophores, the poled order is thermodynamically unstable, especially at elevated temperatures. To avoid the randomization of the poled order, NLO chromophores are usually incorporated into high glass transition temperature (T_g) polymers and/or crosslinked polymer networks [7–13].

In the past decade, polyurethanes have been extensively investigated and shown potential in the fabrication of devices due to ease of synthesis and excellent compatibility with high μβ chromophores [14–21]. Dalton et al. have thoroughly studied a polyurethane system based on toluene-2,4-diisocyanate (TDI) and triethanolamine (TEA) [14–17]. The dynamic stability of dilinkable chromophore incorporated TDI/TEA polyurethane EO material is around 90 °C.

Carbodiimide (CDI) chemistry has been extensively used in peptide synthesis [22,23]. In esterification chemistry, researchers have discovered that its use has been hampered by a side reaction that converts carboxylic acids to *N*-acylureas (Scheme 1) [24]. On the basis of this reaction, a poly-CDI system was developed and subsequently trimellitic anhydride

* Corresponding author.
** Corresponding author. Tel.: +886 4 22852581; fax: +886 4 22854734.
E-mail address: rjjeng@nchu.edu.tw (R.-J. Jeng).

0032-3861/$ - see front matter © 2007 Elsevier Ltd. All rights reserved.
doi:10.1016/j.polymer.2007.02.010

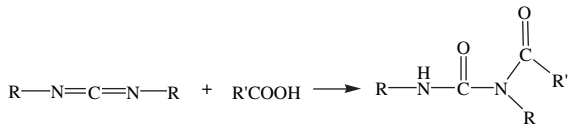

Scheme 1. Formation of acylurea group via the reaction between carbodiimide and carboxylic acid.

(TMA) was added to obtain poly(*N*-acylurea) as the intermediate of the NLO polymer. As the reaction temperature was increased up to 150 °C, poly(*N*-acylurea) would selectively decompose to form isocyanate and amide, and the isocyanate moieties would then react with the carboxylic acid from anhydride to form thermally stable amide–imide linkage. This process is based on a mechanism of sequential self-repetitive reaction (SSRR) [25]. The SSRR methodology is carried out at a more moderate temperature (comparing with the synthesis of polyamide (~220 °C) and polyimide (~250 °C)). Therefore, these poly(amide–imide)s would exhibit better NLO properties because of higher poling efficiency [26–28].

In this study, we have developed a new methodology that introduces the amide–imide units into the main chains of polyurethanes/polyureas. A series of NLO materials containing amide–imide linkages have been prepared via SSRR of CDI derivatives. The intermediate, poly(*N*-acylurea), exhibits excellent organosolubility, which enables the fabrication of high quality optical thin films. Moreover, its moderate glass transition temperature (T_g) characteristic allows the NLO-active polymers to exhibit high poling efficiency. After in situ poling and curing process, *N*-acylurea moieties were converted to amide–imide structures and subsequently the T_g would elevate significantly. The high poling efficiency and good temporal stability could be achieved via SSRR.

2. Experimental

2.1. Materials and measurements

Compounds 1,3-dimethyl-3-phospholene oxide (DMPO) (Hochest), *m*-phenylenediamine (Aldrich), *p*-nitroaniline (Aldrich), trimellitic anhydride (TMA) (Aldrich), sodium nitrite ($NaNO_2$) (Sigma–Aldrich), 4,4′-methylene-diphenylisocyanate (MDI) (Acros), phenyl isocyanate (Lancaster), disperse red 19 (DR19) (Acros) and disperse orange 3 (DO3) (Acros) were used as received. The solvents were purified by distillation under reduced pressure over calcium hydride. Infrared spectra were recorded on a Perkin–Elmer Paragon 500 FT-IR spectrophotometer. ^{1}H NMR characterization was carried out on a Varian Gemini200 NMR Spectrometer in DMSO-d_6 or acetone-d_6. Elemental analysis (EA) was performed on an F002 Heraeus CHN–O Rapid Elemental Analyzer employing acetanilide as a standard. Differential scanning calorimetry (DSC) and thermogravimetric analysis (TGA) were performed on a Seiko SII model SSC/5200 at a heating rate of 10 °C/min under nitrogen and air atmospheres, respectively. Thermal degradation temperature (T_d) is taken at 5% weight loss. UV–vis spectra were recorded on a Perkin–Elmer Lambda 2S Spectrophotometer. A gel permeation chromatograph (Analytical Scientific Instruments Model 500) with a reflection index (RI) detector (Schambeck RI2000) and two columns of Jordi gel DVB mixed bed and 10,000 Å bed in series at 30 °C was used to measure the molecular weight relative to polystyrene standards. The calibration curve was obtained by eight standards in the molecular weight range 3420–2.57×10^6. The carrier solvent was DMF at a flow rate of 1 mL/min. The indices of refraction were measured by a prim coupler (Metricon 2010, at 830 nm) [29,30]. The thicknesses of the polymer films were analyzed by atomic force microscopy (AFM) (Seiko SPI3800N, Series SPA-400).

2.2. Synthesis of 4-(4′-nitrophenyl-diazenyl) phenyl-1,3-diamine (NDPD; Scheme 2) [31]

Under nitrogen atmosphere, 5.5 mmol of *m*-phenylenediamine was added to 1 mL of concentrated hydrochloric acid and 10 mL of water to make salt solution. A mixed paste of *p*-nitroaniline (5.5 mmol), 10 mL of H_2O, and 5.5 mmol $NaNO_2$ was poured into a mixture of crushed ice and 1.5 mL of concentrated hydrochloric acid. The reaction was carried out in an ice bath for 0.5 h. The diazonium salt solution was added slowly into the solution of *m*-phenylenediamine salt with stirring, and the mixture was allowed to react for 1 h. After neutralization with ammonia water for 0.5 h, the product was filtered and washed with water to pH = 5–6. The compound was purified on a silica gel column with the eluent, ethyl acetate/hexane (1/1).

Yield: 89%. Melting point (mp): 236 °C (DSC). ^{1}H NMR (200 MHz, DMSO-d_6, ppm): 8.26 (d, ArH, 2H, $J = 9$ Hz), 7.84 (d, ArH, 2H, $J = 8.8$ Hz), 7.4 (d, ArH, 1H, $J = 9$ Hz), 6.09 (d, ArH, 1H, $J = 9$ Hz), 5.85 (s, ArH, 1H), 6.44 (s, $-NH_2$, 4H). FT-IR (KBr): 3488–3386 cm^{-1} ($-NH_2$), 1502 cm^{-1} and 1336 cm^{-1} ($-NO_2$). $C_{12}H_{11}N_5O_2$: Calcd C 56.03%, H 4.31%, N 27.22%; Found C 55.80%, H 4.52%, N 26.21%.

2.3. Synthesis of 2,4-diamino-4′-(4-nitrophenyl-diazenyl) azobenzene (DNDA; Scheme 2) [31,32]

DNDA was synthesized in the same manner as NDPD. DO3 (1 mmol), $NaNO_2$ (1 mmol), 15 mL of ice water, and 15 mL of dimethyl sulfoxide (DMSO) were mixed with 5.5 mL of concentrated hydrochloric acid. The mixture was stirred for 0.5 h in an ice bath and then slowly poured into a solution containing 1.5 mmol of *m*-phenylenediamine and 36 mL of methanol/water cosolvent (2/1 in volume ratio). The mixture was stirred vigorously for 1 h and then neutralized with sodium acetate to pH 5–6. After further stirring for 0.5 h, the mixture was filtered. Subsequently, the precipitate was dried.

Yield: 88%. Mp: 224 °C (DSC). ^{1}H NMR (200 MHz, DMSO-d_6, ppm): 8.43 (d, ArH, 2H, $J = 8.4$ Hz), 8.03 (t, ArH, 4H, $J = 8.7$ Hz), 7.89 (d, ArH, 2H, $J = 8.8$ Hz), 7.42 (d, ArH, 1H, $J = 8.6$ Hz), 6.09 (d, ArH, 1H, $J = 8.2$ Hz), 5.86 (s, ArH, 1H), 6.29 (s, $-NH_2$, 4H). FT-IR (KBr): 3480–3392 cm^{-1} ($-NH_2$), 1514–1342 cm^{-1} ($-NO_2$). $C_{18}H_{15}N_7O_2$:

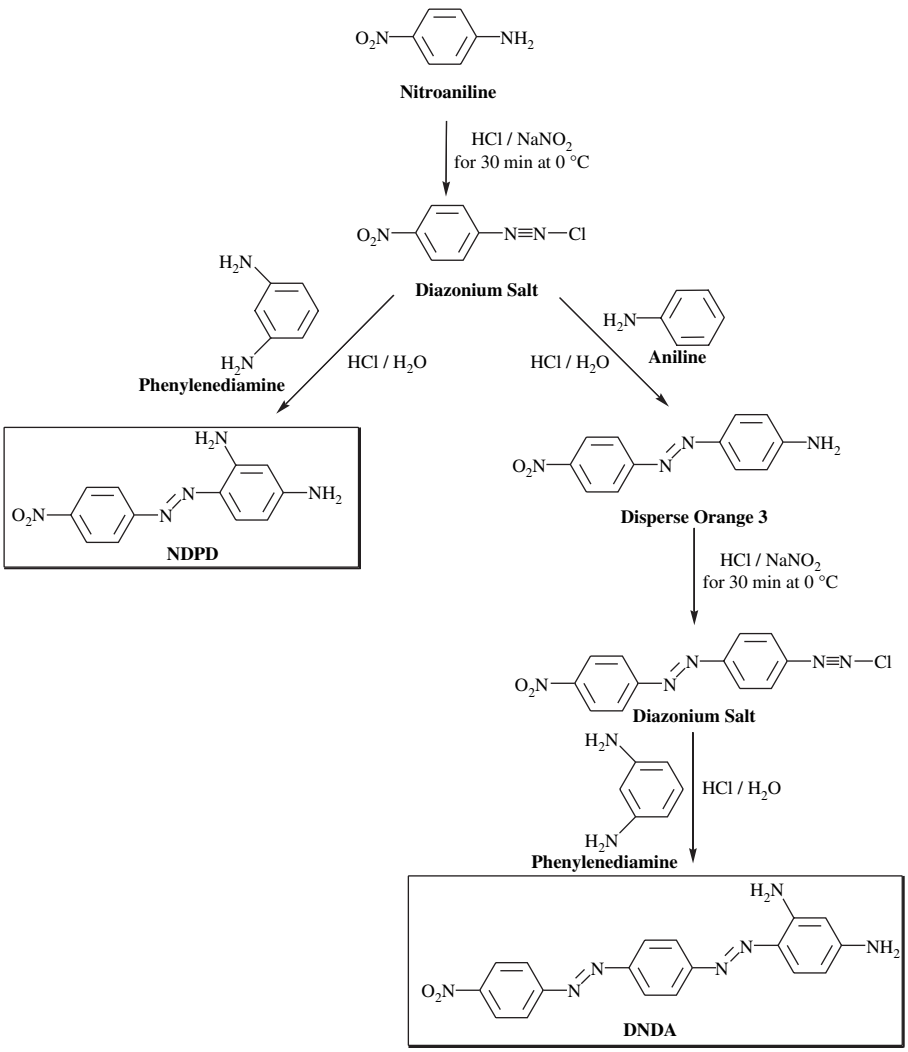

Scheme 2. Synthesis of the azobenzene dyes (NDPD and DNDA).

Calcd C 59.83%, H 4.18%, N 27.13%; Found C 59.35%, H 4.54%, N 26.48%.

2.4. Preparation of the polyacylurea-DR19 (PaDR; Scheme 3)

Under nitrogen atmosphere, DR19 (1 mmol) was dissolved in anhydrous THF (5 mL) at room temperature, which was followed by the immediate addition of MDI (4 mmol). The solution was stirred at 60 °C for 2 h. After adding 1,3-dimethyl-3-phospholene oxide (DMPO) and phenyl isocyanate (0.67 mmol), poly-CDI was obtained. Phenyl isocyanate served as an end-capping agent to ensure the poly-CDI soluble with a reasonable molecular weight. Subsequently, TMA (1.5 mmol) was added to the poly-CDI solution. The solution was kept at 60 °C for another 6 h. After removing THF under vacuum, a polyacylurea, PaDR61 was obtained. Other polyacylurea-DR19 samples were also prepared in the same manner (PaDR samples; Table 1). The molecular weight of the polymer was determined by GPC. The chromatogram of PaDR61 indicated that the number average molecular weight (M_n) value and polydispersity were 169,400 and 1.34, respectively.

2.5. Preparation of the polyacylurea-NDPD (PaND; Scheme 4)

NDPD (1 mmol) was dissolved in anhydrous THF (5 mL) at room temperature, which was followed by the immediate addition of MDI (4 mmol). The solution was stirred at 60 °C for 2 h. After adding DMPO, poly-CDI was obtained. Subsequently, TMA (1.5 mmol) was added to the poly-CDI solution. The solution was kept at 60 °C for another 6 h. After removing THF under vacuum, a polyacylurea, PaND41 was obtained. Other polyacylurea-NDPD samples were also prepared in the same manner (PaND samples; Table 1). The M_n value and polydispersity of PaND61 were 90,000 and 3.75, respectively.

2.6. Preparation of the polyacylurea-DNDA (PaDN; Scheme 4)

DNDA (1 mmol) was dissolved in anhydrous DMF (5 mL) at room temperature, which was followed by the immediate addition of MDI (4 mmol). The solution was stirred at 60 °C for 2 h. After adding DMPO, poly-CDI was obtained. Subsequently, TMA (1.5 mmol) was added to the poly-CDI solution.

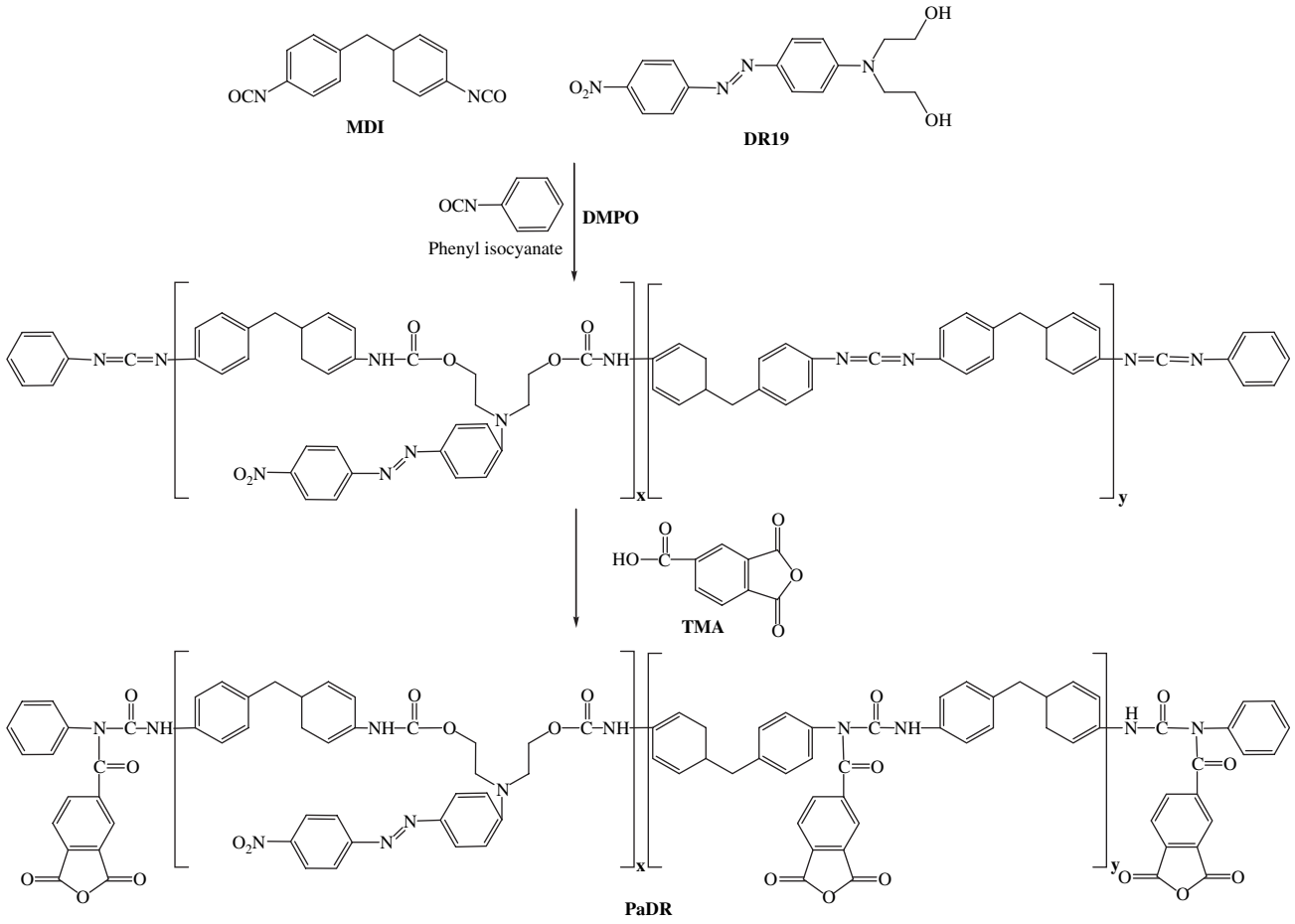

Scheme 3. Synthesis of PaDR.

The solution was kept at 60 °C for another 6 h. After removing THF under vacuum, a polyacylurea, PaDN41 was obtained. Other polyacylurea-DNDA samples were also prepared in the same manner (PaDN samples; Table 1). The M_n value and polydispersity of PaDN61 were 54,200 and 3.08, respectively.

Table 1
Compositions of the NLO materials based on poly(amide–imide)s

Feed ratio	Feed molar ratio	Real molar ratio[a]	Sample	
			Before curing	After curing
MDI/Ph-NCO = 6/1	0.30	0.29	PaDR61	PIDR61
MDI/Ph-NCO = 8/1	0.31	0.31	PaDR81	PIDR81
MDI/Ph-NCO = 10/1	0.31	0.30	PaDR101	PIDR101
MDI/dye = 2/1	1.00	0.99	PaND21	PIND21
MDI/dye = 4/1	0.33	0.32	PaND41	PIND41
MDI/dye = 6/1	0.20	0.20	PaND61	PIND61
MDI/dye = 8/1	0.14	0.14	PaND81	PIND81
MDI/dye = 2/1	1.00	0.99	PaDN21	PIDN21
MDI/dye = 4/1	0.33	0.33	PaDN41	PIDN41
MDI/dye = 6/1	0.20	0.19	PaDN61	PIDN61
MDI/dye = 8/1	0.14	0.14	PaDN81	PIDN81
MDI/dye = 10/1	0.11	0.11	PaDN101	PIDN101

[a] The real molar ratios (x/y) of copolymers could be further calculated by the following equations: $x + y = 1$ and $(\text{dye} - \text{cont.})\% = (x \times (M_{dye}))/(x \times (M_{dye} + M_{MDI}) + y \times (M_{MDI} \times 2 + M_{TMA})) \times 100\%$; M_{MDI}, the molecular weight of MDI; M_{dye}, the molecular weight of dye; M_{TMA}, the molecular weight of TMA.

2.7. Preparation of the poly(amide–imide)s (PIDR, PIND, PIDN; Scheme 5)

To obtain the poly(amide–imide)s (PIDR, PIND and PIDN samples; Table 1), the polyacylureas were thermally treated at 200 °C for 2 h. SSRR was performed during this period of thermal treatment [25].

2.8. Thin film preparation

To prepare the second-order NLO polymer films, the polyacylureas were, respectively, dissolved in DMF. The polymer solution was stirred at room temperature for 3 h and filtered through a 0.45 μm filter. Thin films were prepared by spin coating the filtered polymer solution onto indium tin oxide (ITO) glass substrates. Prior to the poling process, these thin films were dried in vacuum at 60 °C for 24 h.

2.9. Poling process, electro-optical (EO) coefficient (r_{33}) and optical loss measurement

EO coefficients of the poled samples were measured at 830 nm wavelength using the simple reflection technique [33]. The poling process for the second-order NLO polymer films was carried out using an in situ contact poling technique.

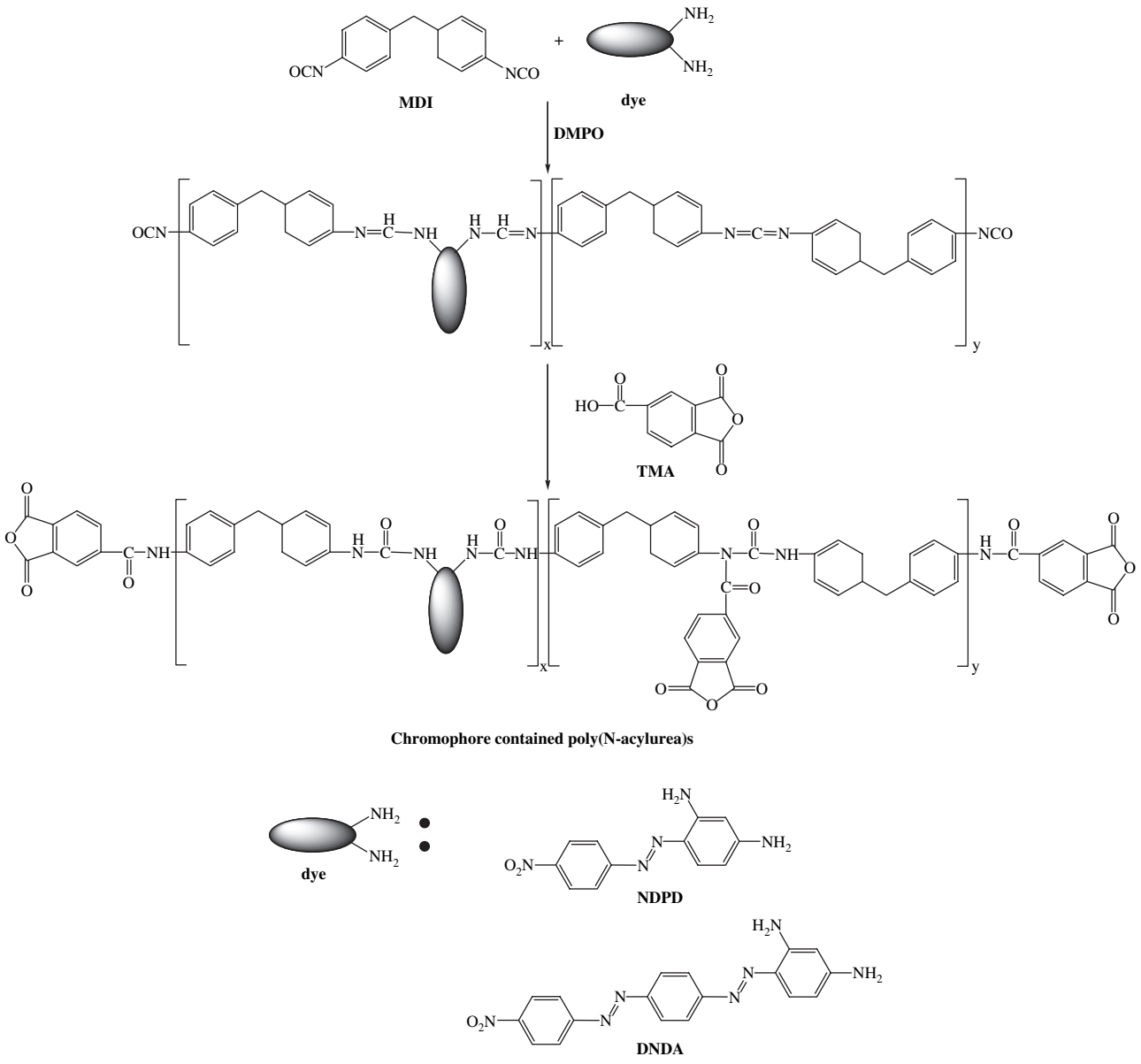

Scheme 4. Synthesis of PaND and PaDN.

The poling voltage was maintained at 70 V and the temperature was kept at 200 °C for 2 h. The formation of the amide–imide linkages via SSRR, and the alignment of chromophores proceeded simultaneously during this period. Upon saturation of the EO signal intensity, the sample was then cooled down to room temperature in the presence of the poling field at which point the poling field was terminated. Optical losses of the polymer waveguides for the poly(amide–imide)s were measured according to the literature (Scheme 6) [34]. The laser beam (830 nm) first passes through a linear polarizer and a polarizing beam splitter, thus removing the noise caused by polarizing fluctuations in the laser output. Rotation of the linear polarizer allows the intensity of the beam to be adjusted while rotation of the beam splitter allows for selection of TE polarized light. The unreflected beam is focused onto a prism coupler that is mounted on a rotation stage. The scattered light is imaged with an infrared-sensitive charge-injection-device camera system. A distance scale is provided by imaging a ruler to provide a scale in pixels per centimeter. A statistical linear fit of the data to the logarithm of the scattered light intensity versus the distance propagated down the waveguide would yield a waveguide loss as a slope.

3. Results and discussion

The reaction conditions of the NLO-active intermediates were determined using DSC reaction scans (Fig. 1). The SSRR of PaDR started at 110 °C and peaked at 180 °C. For the PaND, the reaction started at 98 °C and peaked at 172 °C. Moreover, for the PaDN, the reaction started at 90 °C and peaked at 185 °C. The exothermic peaks appeared at around 140 °C indicates that poly(*N*-acylurea) decomposed

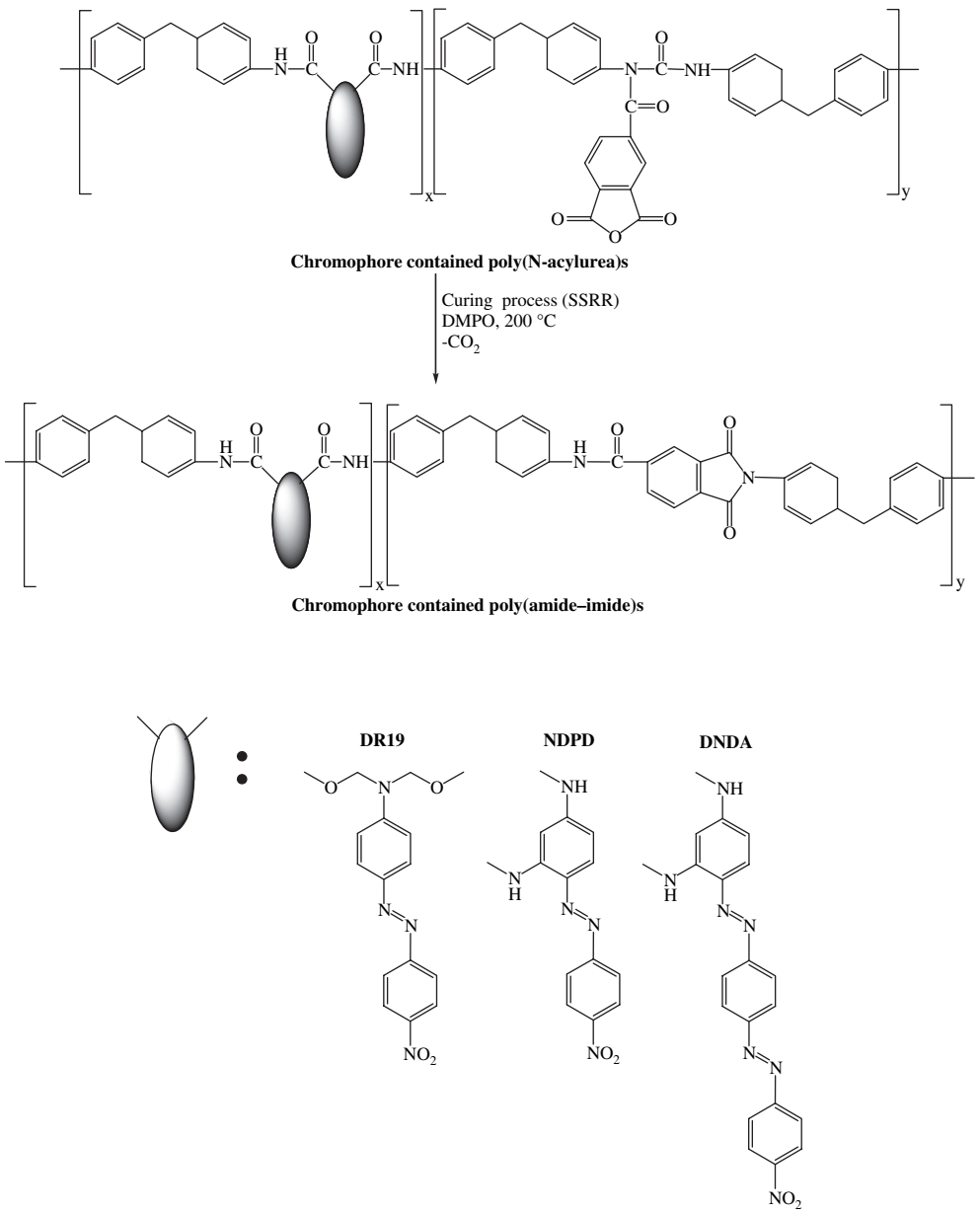

Scheme 5. Synthesis of poly(amide−imide)s consisting of DR19, NDPD, or DNDA.

rapidly into fragments consisting of isocyanates and amides. When the reaction temperature reached 170 °C (valley point), the decomposition of poly(*N*-acylurea) was complete. As the temperature further raised to the starting point of another exothermic peak (approximately 190 °C), a ring-closure step to yield poly(amide−imide) started to proceed [25]. As the temperature further increased to 225 °C, the reaction scans were terminated due to the consideration of the azo chromophore degradation [35]. Based on the above, and the consideration, an optimized curing condition for all of the NLO-active poly(*N*-acylurea)s was chosen as follows: the polymer films were pre-cured at 150 °C for 0.5 h. The poling temperature was slowly raised to 200 °C (5 °C/min). The samples were then cured at 200 °C for 1.5 h. As a result, the poly(amide−imide)s were formed via SSRR. To avoid degradation of the NLO-active chromophores (DR19, NDPD, and DNDA) during poling, an UV−vis spectrophotometer was utilized to trace the chromophore (DR19) in the poly(amide−imide)s. The absorption maxima of the NLO-active polymer film were obtained

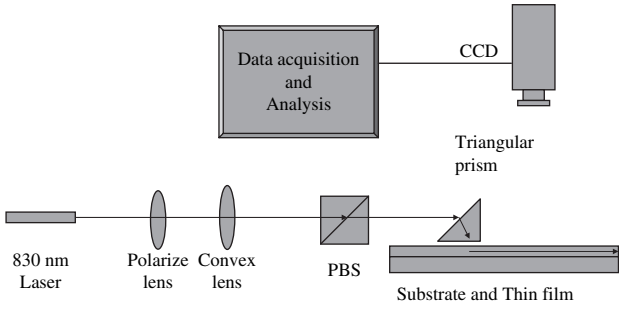

Scheme 6. Schematic of equipment for measuring the mode propagation losses of planar optical waveguides.

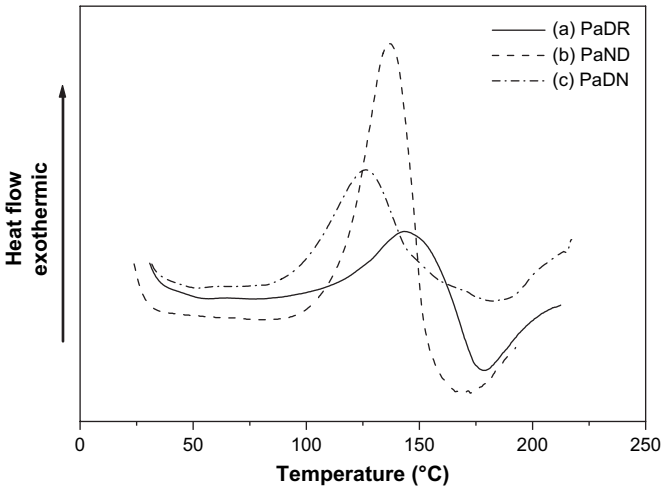

Fig. 1. DSC thermograms of polyacylureas: (a) PaDR, (b) PaND, and (c) PaDN.

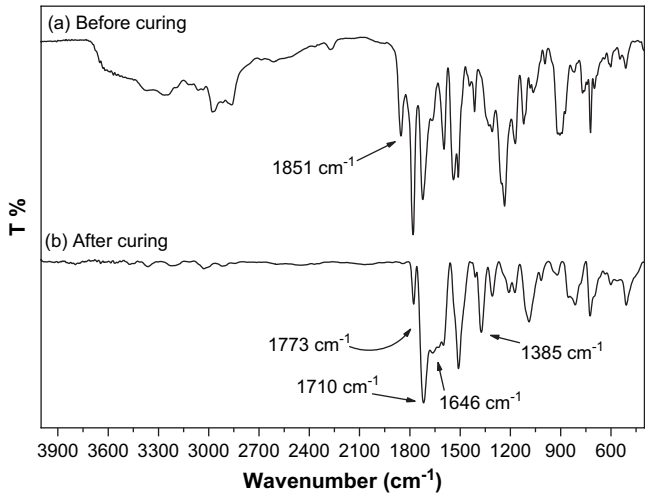

Fig. 2. Infrared spectra of the (a) PaDR and (b) cured PaDR, i.e. PIDR.

after thermal treatment at various temperatures (10 °C per ramp; from 30 to 250 °C) for 2 h. A sharp decrease of the chromophore absorbance was observed when temperatures were higher than 210 °C. This indicates that chromophores are capable of enduring thermal treatment at temperatures lower than 210 °C. Therefore, to avoid the damages of thermal treatment and electric field, the poling temperature should be confined under 210 °C. However, thermal treatment experiments seem not to provide enough information for the optimizing poling conditions. One has to take the reaction chemistry into account when the poling and curing processes would proceed simultaneously in this system. As mentioned earlier, the optimized curing temperature was chosen to 200 °C. To obtain optimized electric field for poling, the EO coefficient of the sample was traced under various poling voltages at 200 °C. It was found that the largest optical nonlinearity could be obtained while poling at 200 °C under 70 V. On the basis of these results, an optimized poling process was chosen as follows: the optimized contacted poling voltage was 70 V and the temperature was kept at 150 °C for 0.5 h and then poled at 200 °C for 1.5 h. The formation of poly(amide–imide) and the molecular alignment of the poled order proceeded simultaneously during this period.

FT-IR was utilized to monitor the SSRR process. FT-IR spectra of the PaDR and its cured sample are shown in Fig. 2. The sharp absorption peaks at around 1720 cm^{-1}, 1780 cm^{-1}, and 1385 cm^{-1} were identified as the formation of polyimide for the cured sample. Those peaks at around 1646 cm^{-1} and 3300–3400 cm^{-1} were identified as the presence of amide groups. The completion of SSRR process was also indicated by the disappearance of anhydride absorption peak at around 1851 cm^{-1}. The FT-IR results demonstrate that the SSRR process proceeded successfully to form poly(amide–imide)s during the optimized curing/poling process.

To further confirm the cured poly(amide–imide) structure, ^{1}H NMR analysis on two model compounds was performed. This is because of insolubility of the cured NLO-active poly(amide–imide)s. Model compound M1 with acylurea group underwent SSRR process (200 °C, 1.5 h) to form model compound M2 with amide–imide group (Scheme 7). The ^{1}H NMR analysis data confirm the formation of amide–imide structure [36].

The solubility of all poly(*N*-acylurea) samples is excellent with common organic solvents such as THF, DMF, DMAc, and DMSO. Because of the excellent organosolubility, these poly(*N*-acylurea)s could be easily processed into optical quality thin films by spin coating. Moreover, all of the NLO-active poly(amide–imide)s exhibited great solvent resistance after SSRR process.

Thermal properties of the chromophore-containing amide–imide-based polymers are shown in Table 2. The T_g values of these polymers were measured using DSC after the above-mentioned curing (SSRR) process. For the PIDR samples, T_g values ranging from 175 to 210 °C were obtained. The T_g values of the PIND samples were in the range between 150 and 197 °C, whereas T_g values ranging from 150 to 210 °C were obtained for the PIDN samples. The T_g values of PIDR samples increased with increasing MDI content. This indicates that the T_g value was enhanced by the incorporation of higher content of carbodiimide, leading to higher content of amide–imide linkages. As the content of MDI increased, the T_g values of PIND and PIDN behaved like a parabolic curve. These two series of samples exhibited maximum points at the ratios (MDI/chromophore) of 4/1 and 6/1, respectively. This indicates that the T_g value was enhanced by the incorporation of higher imide ratio at first. However, it seems that the polymers with higher acylurea contents could not be completely cured to form imide groups under the same thermal treatment. As a result, this led to the decrease of T_g. It is important to note that the T_gs of the polymer intermediates, poly-CDIs, are approximately 120–140 °C, whereas the T_gs of the NLO-active poly(amide–imide)s are in the range between 150 and 210 °C. The T_gs of the NLO-active polymers were elevated significantly after the in situ poling and curing process. The moderate T_g characteristic of poly-CDIs allowed the NLO-active polymers to exhibit high poling efficiency. After in situ poling and

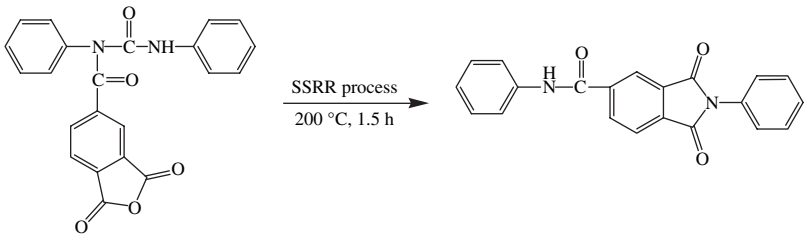

M1 M2

Scheme 7. SSRR process of the model compounds M1 and M2.

Table 2
Thermal properties of the poly(amide–imide) based NLO materials

Sample	T_g (°C)	T_d[a] (°C)
PIDR61	175	369
PIDR81	200	392
PIDR101	210	347
PIND21	150	255
PIND41	197	284
PIND61	190	292
PIND81	192	311
PIDN21	150	265
PIDN41	210	266
PIDN61	190	282
PIDN81	191	269
PIDN101	170	295

[a] T_d was read at the temperature corresponding to 5% weight loss by TGA.

curing process (SSRR), the T_gs would elevate significantly because the *N*-acylurea moieties were converted to amide–imide structures. As a result, good temporal stability could be achieved. In addition, thermal decomposition behavior was measured using TGA under nitrogen. The T_d value was read at the temperature corresponding to the weight loss of 5%. The T_d values of the cured PIDR, PIND and PIDN samples are also summarized in Table 2. The T_d values were observed at temperatures above 260 °C for all NLO-active poly(amide–imide)s.

The absorption characteristics of polymer films have been investigated by UV–vis spectroscopy (Table 3). The maximum of the absorption was located around 530 nm for the PIDR films, whereas the cut-off wavelength was 780 nm. The PIND films exhibited the absorption maximum and cut-off wavelength at 454 nm and 611 nm, respectively. For the PIDN films, the maximum of the absorption was located around 485 nm and the cut-off wavelength was 649 nm. Because of the longer π-conjugated length of the DNDA chromophore, a red shift was obtained for the PIDN samples as compared to the PIND sample. In addition, the NLO properties were measured at 830 nm in order to circumvent the absorption range.

Table 3
UV–vis absorption properties of poly(amide–imide) films

	λ_{max} (nm)	$\lambda_{cut\text{-}off}$ (nm)
PIDR	530	780
PIND	454	611
PIDN	485	649

Optical properties of these NLO materials are shown in Table 4. Thicknesses of the polymer films range from 0.6 to 1.1 μm, whereas refraction indices range from 1.66 to 1.77. EO coefficients resulted from the in situ poling process are in the range from 5.2 to 25.2 pm/V (measured at 830 nm), depending upon the chromophore concentrations. Optical nonlinearity plotted as a function of real chromophore content is shown in Fig. 3. It is important to note that the real chromophore contents were determined by UV–vis investigations

Table 4
Optical properties of poly(amide–imide) based NLO materials

Sample	Chromophore content[a] (wt%)	d[b] (μm)	Refraction indices	Optical loss (dB/cm) at 830 nm	r_{33} (pm/V)
PIDR61	15.4	1.0	1.76	–	7.5
PIDR81	16.0	0.6	1.76	–	4.3
PIDR101	16.9	1.0	1.73	–	4.7
PIND21	27.1	0.7	1.77	6.6	8.1
PIND41	14.0	0.6	1.75	5.9	7.5
PIND61	9.5	0.8	1.75	4.6	6.3
PIND81	7.1	0.8	1.75	5.7	5.7
PIDN21	31.4	1.1	1.66	5.3	25.2
PIDN41	18.6	0.7	1.74	5.4	15.3
PIDN61	12.8	0.6	1.75	5.2	20.1
PIDN81	9.7	0.6	1.76	3.8	13.0
PIDN101	7.9	0.9	1.75	4.1	5.2

[a] Determined by UV–vis investigations.
[b] d is the thickness of the polymer film.

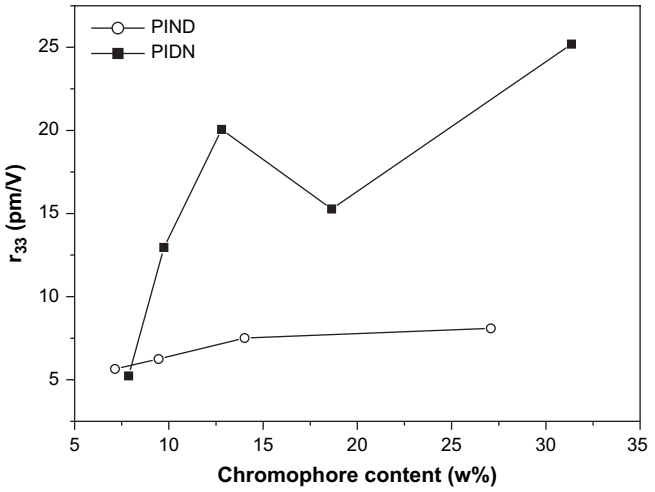

Fig. 3. EO coefficient plotted as a function of chromophore content for these NLO materials.

[37–42]. The r_{33} values of all polymers are proportional to their chromophore contents, except for the highest T_g sample, PIDN41. This is possibly due to the fact that a high poling efficiency is difficult to obtain for the high T_g polymers due to increased chain entanglement [43]. Nevertheless, this problem was somewhat circumvented via the two-step simultaneous poling and curing process in the work. In general, the larger values of EO coefficients were obtained by the PIDN samples containing the DNDA chromophores with the longer conjugated linkages [44]. This series of NLO poly(amide–imide)s prepared via SSRR of CDI derivatives allow the chromophores to orient easily towards electric direction prior to curing. As a result, larger EO coefficients were obtained. In one example, PIDN61 with a chromophore content of 12.8 wt% exhibited a r_{33} of 20 pm/V. Yu and co-workers [45] reported the preparation of stable NLO copolyimides via traditional imidization between diamino-chromophore and dianhydride. This series of copolyimides with a similar chromophore content (14.4 wt%) exhibited a relatively smaller EO coefficient.

In general, the EO coefficient of NLO polymers remains stable at low temperatures, but decays significantly at a specific temperature. This specific temperature is defined as the effective relaxation temperature [1]. This value provides information on maximum device operating temperatures that the film can endure, and allows quick evaluation of the temporal and thermal stability of the materials. In this study, the PIDN41 sample exhibits higher effective relaxation temperature (170 °C) as compared to both PIDR81 (130 °C) and PIND41 (160 °C) samples. As mentioned previously, the T_g values of these three series of poly(amide–imide) samples are in the similar range. In spite of this, their effective relaxation temperatures are quite different. This is due to the difference of tether groups and conjugation lengths of the chromophores. The PIDN sample consists of the chromophore with longest conjugation length (DNDA), whereas the PIDR sample consists of the chromophore (DR19) with flexible tether groups.

Fig. 4 shows the temporal stability of EO coefficient for the poled/cured samples at 80 °C for 100 h. A much better temporal stability was obtained for the poled/cured PIDN sample as compared to the poled/cured PIND sample. After being subjected to thermal treatment at 80 °C for 100 h, almost no decay in EO coefficient was observed for the poled/cured PIDN61 sample. Moreover, better temporal stability was obtained for the samples with the DNDA and NDPD chromophores. This indicates that the samples with the DR19 chromophore consisting of more flexible ethylene–urethane linkage would decrease the temporal stability of EO coefficient, despite their higher molecular weights and high T_gs.

In the investigation of optical loss, only the samples with better temporal stability (PIND and PIDN) were measured at 830 nm under TE guide modes. As shown in Table 4, the optical losses of these poly(amide–imide) NLO polymer waveguides are in the range 3.8–6.6 dB/cm. It is important to note that the poly(amide–imide) containing PIND61 exhibits smaller optical loss than the rest of samples in PIND series. Similar phenomenon was also observed for PIDN81 in PIDN series. The number density of C–H, O–H and N–H bonds in the intrinsic structures plays a key role in lowering the optical loss of materials [26,30]. There are two possible reasons for the above trend: (a) the reduction of chromophore density in the polymer causes optical loss to reduce; (b) the raise of the amide–imide ratio leads to increased optical loss, especially for higher amide–imide content [21].

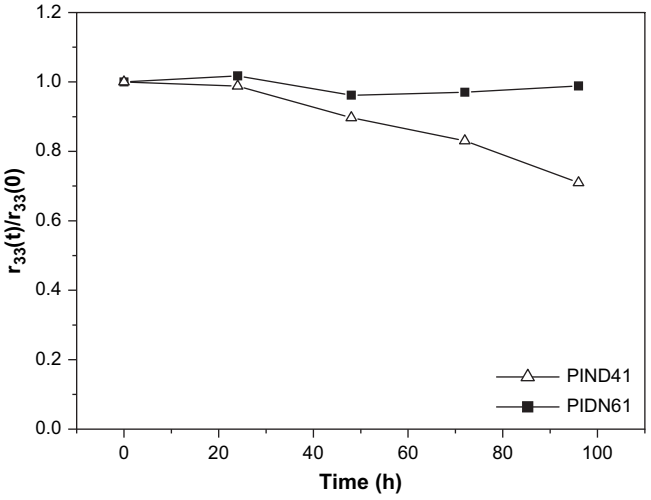

Fig. 4. Temporal behavior of the EO coefficient for the poled/cured PIND and PIDN samples at 80 °C.

4. Conclusion

The NLO poly(amide–imide)s were prepared by the intermediate, poly(*N*-acylurea), via SSRR. These thermally stable NLO poly(amide–imide)s ($T_g = 150–210$ °C) exhibited high poling efficiency ($r_{33} = 4.3–25.2$ pm/V, measured at 830 nm). The intermediate, poly(*N*-acylurea), exhibits high solubility which enables the fabrication of high quality thin films. Moreover, all of the NLO materials have shown solvent resistance and waveguide properties after curing process. Not only the high poling efficiency could be obtained, but the temporal stability at 80 °C was also achieved after curing process, i.e. the formation of amide–imide linkages.

Acknowledgements

Financial support from National Science Council of Taiwan and Chung-Shan Institute of Science and Technology is gratefully acknowledged. The authors also thank Education Ministry of Taiwan for funding Center for Advanced Industry Technology and Precision Processing, NCHU.

References

[1] Prasad PN, Williams DJ. Introduction to nonlinear optical effects in molecules and polymers. New York: Wiley; 1991.
[2] Chang CC, Chen CP, Chou CC, Kuo WJ, Jeng RJ. J Macro Sci Polym Rev 2005;45:125–70.
[3] Singer KD, Sohn JE, Lalama SJ. Appl Phys Lett 1986;49:248.

[4] Sinyukov AM, Leahy MR, Hayden LM, Haller M, Luo J, Jen AKY, et al. Appl Phys Lett 2004;85:5827–9.
[5] Baehr JT, Hochberg M, Wang G, Lawson R, Liao Y, Sullivan PA, et al. Opt Express 2005;13:5216–26.
[6] Chemala DS, Zyss J, editors. Nonlinear optical properties of organic molecules and crystals. New York: Academic Press; 1987.
[7] Tsutsumi N, Morishima M, Sakai W. Macromolecules 1998;31:7764–9.
[8] Chen CP, Huang GS, Jeng RJ, Chou CC, Su WC, Chang HL. Polym Adv Technol 2004;15:587–92.
[9] Jeng RJ, Jan LH, Lee RH. J Macromol Sci Pure Appl Chem 2001;A38:821–37.
[10] Jeng RJ, Chan LH, Lee RH, Hsiue GH, Chang HL. J Macromol Sci Pure Appl Chem 2001;A38:1259–74.
[11] Kuo WJ, Hsiue GH, Jeng RJ. J Mater Chem 2002;12:868–78.
[12] Jeng RJ, Hong WY, Chen CP, Hsiue GH. Polym Adv Technol 2003;14:66–75.
[13] Jeng RJ, Chang CC, Chen CP, Chen CT, Su WC. Polymer 2003;44:143–55.
[14] Chen M, Yu L, Dalton LR, Shi Y, Steier WH. Macromolecules 1991;24:5421–8.
[15] Chen M, Dalton LR, Yu LP, Shi YQ, Steier WH. Macromolecules 1992;25:4032–5.
[16] Mao SSH, Ra Y, Guo L, Zhang C, Dalton LR. Chem Mater 1998;10:146–55.
[17] Harper AW, Mao SSH, Ra Y, Zhang C, Zhu J, Dalton LR. Chem Mater 1999;11:2886–91.
[18] Zhang C, Wang C, Yang J, Dalton LR, Sun G, Zhang H, et al. Macromolecules 2001;34:235–43.
[19] Kuo WJ, Hsiue GH, Jeng RJ. Macromolecules 2001;34:2373–84.
[20] Kuo WJ, Hsiue GH, Jeng RJ. Macromol Rapid Commun 2001;22: 601–6.
[21] Wang C, Zhang C, Lee MS, Dalton LR, Zhang H, Steier WH. Macromolecules 2001;34:2359–63.
[22] Wendlberger G. Houben–Weyl methoden der organischen chemie, part 2, vol. 15. Stuttgart: Thieme Verlag; 1974. p. 103.
[23] Toru J, Hiroyuki W, Hiroo T. J Mol Catal B Enzym 2002;17:49–57.
[24] Jeffrey SM, Samuel IS. Macromolecules 1990;23:70–7.
[25] Wei KL, Wu CH, Huang WH, Lin JJ, Dai SHA. Macromolecules 2006;39:12–4.
[26] Besir K. US Patent 4,061,623; 1977.
[27] Yang CP, Chen CP, Woo EM. Polymer 2004;45:5279–93.
[28] Balcerzak ES, Sapich B, Stumpe J. Polymer 2005;46:49–59.
[29] Shi W, Fang CS, Sui Y, Yin J, Pan QW, Gu QT, et al. Opt Commun 2000;183:299.
[30] Shi W, Fang CS, Sui Y, Yin J, Pan QW, Gu QT, et al. Solid State Commun 2000;16:67.
[31] Zhou YM, Leng WN, Liu XO, Xu QH, Feng JK, Liu JH. J Polym Sci Polym Chem 2002;40:2478–86.
[32] Wang WJ, Chin WK, Wang WJ. J Polym Sci Part B Polym Phys 2002;40:1690–703.
[33] Teng CC, Man HT. Appl Phys Lett 1990;56:1734.
[34] Jeng RJ, Hsiue GH, Chen JI, Marturunkakul S, Li L, Jiang XL, et al. J Appl Polym Sci 1995;55:209–14.
[35] Kuo WJ, Chang MC, Juang TY, Chen CP, Chen CT, Chang HL, et al. Polym Adv Technol 2005;16:515–23.
[36] Note: M1: ^{1}H NMR (600 MHz, acetone, ppm): 7.12 (dt, $J = 7.2$ Hz, 1H), 7.25–7.37 (m, 5H), 7.45 (dd, $J = 8.4$, 0.6 Hz, 2H), 7.60 (d, $J = 8.4$ Hz, 2H), 7.75 (d, $J = 7.8$ Hz, 1H), 7.91 (dd, $J = 6.6$, 1.8 Hz, 2H), 10.80 (br s, 1H); M2: ^{1}H NMR (600 MHz, DMSO, ppm): 7.14 (t, $J = 7.2$ Hz, 1H), 7.38 (t, $J = 7.8$ Hz, 2H), 7.46–7.50 (m, 3H), 7.54 (t, $J = 7.8$ Hz, 2H), 7.82 (d, $J = 7.8$ Hz, 2H), 8.12 (d, $J = 7.8$ Hz, 1H), 8.45 (dd, $J = 7.8$, 1.8 Hz, 1H), 8.54 (s, 1H), 10.64 (s, 1H); Anal. Calcd for $C_{21}H_{14}N_2O_3$: N 8.20%, C 73.70%, H 4.10%. Found N 8.21%, C 73.61%, H 4.18%. Mp: 271–273 °C.
[37] Song N, Men L, Gao JP, Bai Y, Beaudin AMR, Yu G, et al. Chem Mater 2004;16:3708–13.
[38] Luo JD, Haller M, Li HX, Tang HZ, Jen AKY. Macromolecules 2004;37:248–50.
[39] Dorr M, Zentel R. Macromol Rapid Commun 1994;15:935–42.
[40] Balogh DT, Carvalho AJF. J Appl Polym Sci 2007;103:841–7.
[41] Fukuda T, Matsuda H, Shiraga T, Kimura T, Kato M, Viswanathan NK, et al. Macromolecules 2000;33:4220–5.
[42] Yang S, Li L, Cholli AL, Jayant Kumar, Tripathy SK. Biomacromolecules 2003;4:366–71.
[43] Zhang C, Wang CU, Dalton LR. Macromolecules 2001;34:253–61.
[44] Clays K, Coe BJ. Chem Mater 2003;15:642–8.
[45] Yu D, Gharavi A, Yu L. Macromolecules 1996;29:6139–42.